Biochemistry and Biophysics Reports 10 (2017) 1–6

Contents lists available at ScienceDirect

Biochemistry and Biophysics Reports

journal homepage: www.elsevier.com/locate/bbrep

Peptide oligomers from ultra-short peptides using sortase

Natalya Voloshchuk, Long Chen, Qiang Li, Jun F. Liang*

Department of Chemistry, Chemical Biology, and Biomedical Engineering, Charles V. Schaefer School of Engineering and Sciences, Stevens Institute of Technology, Hoboken, NJ 07030, USA

ARTICLE INFO

Keywords:
Peptide oligomer
Ultra-short peptide
Ligation
Cyclic peptide
Sortase

ABSTRACT

Sortase A catalyzed ligation of ultra-short peptides leads to inter/intra-molecular transpeptidation to form either linear or cyclic oligomers dependent upon the peptide length. Cyclic peptides were the main products for peptides with more than 15aa. However, for ultra-short (< 15aa) peptides, cyclic oligomers became predominant in prolonged reactions. Peptides with 1–3 aminoglycines were equally active but peptide oligomers from peptide containing more than one aminoglycine were prone to hydrolysis.

1. Introduction

Bioactive peptides have many unique and unbeatable features in comparison with proteins and other synthesized polymers. Bioactive peptides regulate many physiological processes, acting at some sites as endocrine or paracrine signals and at others as neurotransmitters or growth factors [1], and show useful properties for human health, including antimicrobial, antifungal, antiviral, and antitumor activities [2,3]. In addition, peptides can interact specifically with toxic metal ions to act as effective chelating agents [4,5], and peptides with specific sequences can self assemble to form materials with regular nanostructures [6–8]. Although most peptides can be produced using the molecular biology approach, they are produced in limited quantities at high costs and associated with some difficulties in purification and isolation. In addition, some peptides with special structures, such as cyclic peptides, can hardly be produced by the biological method. This is especially true for the biomedical applications in which long peptides with functional sequences are usually needed [8].

Staphylococcus aureus Sortase A ($SrtA_{Staph}$), a cysteine transpeptidase, recognizes an LPXTG motif near C-terminus of a protein substrate and cleaves the peptide bond between threonine and glycine residues to form a thioacyl enzyme intermediate between the catalytic cysteine and the substrate threonine [9,10]. The intermediate reacts with the N-terminus of an oligoglycine in nucleophilic substitution with formation of amide bond between the substrate threonine and the incoming glycine [11]. This $SrtA_{Staph}$-catalyzed transpeptidation reaction has been used for protein/peptide ligation and labeling [12,13-17,26,27]. Recently, Wu et al. found that Sortase A mediated transpeptidation seemed to be length dependent for peptides with 16–19 amino acids [25]: a cyclic dimer was the major product for peptides with 16 and 17 amino acids while the main product of 19aa peptide was a cyclic monomer. However, $SrtA_{Staph}$-mediated peptide ligation and thus peptide oligomer production using ultra-short (< 15 amino acids) peptides has not been studied.

2. Experimental details

2.1. Peptides

All peptides for this study (> 90% in purity) were synthesized by Genescript Corp. Methyl ester modified peptides (peptide-OMe) were produced according to method reported previously [18]. The replacement of the glycine in the minimal $SrtA_{Staph}$ recognition sequence, LPRT G, by the threonine methyl ester (-OMe) was shown to minimize product hydrolysis [18].

2.2. Sortase a expression and purification

Wild type *Staphylococcus aureus* Sortase A containing residues 60–206 (St-$SrtA_{\Delta 59}$), named as $SrtA_{Staph}$, was produced in *Escherichia coli* (*E. coli*). Plasmid pET15bSt-$SrtA_{\Delta 59}$ (a gift from Dr. Robert Clubb, UCLA) was used for expression. pET15bSt-$SrtA_{\Delta 59}$ was transformed into BL21-Gold(DE3) competent cells (Stratagene, CA). Cultures were grown in 1.0 L of Luria-Bertani (LB) media supplemented with ampicillin (200 μg/mL) at 37 °C with shaking at 250 rpm. After cells were grown to an optical density of 0.6 at 600 nm, 1 mM isopropyl thioglucoside (IPTG, Fisher Scientific) was added to induce protein expression. The expression continued for 3 h at 37 °C. The cells were harvested by centrifugation at 4,000 rpm. Cell pellets were resuspended in the buffer B (20 mM Tris-HCL, pH 7.5, 150 mM NaCl, 15 mM 2-mercaptoethanol)

* Correspondence to: Department of Chemistry, Chemical Biology, and Biomedical Engineering, Stevens Institute of Technology, Castle Point on Hudson, Hoboken, NJ 07030, USA.
E-mail address: jliang2@stevens.edu (J.F. Liang).

http://dx.doi.org/10.1016/j.bbrep.2017.02.005
Received 27 July 2016; Received in revised form 25 January 2017; Accepted 3 February 2017
Available online 20 February 2017

and lysed by sonication. $SrtA_{Staph}$ protein bearing N-terminal His tag was purified by affinity chromatography using a His-Select Nickel Affinity gel (Sigma). Purified protein was eluted with buffer B containing 200 mM imidazole and then concentrated using Amicon Ultra Centrifugal filters (Millipore) with MWCO of 10 kDa. $SrtA_{Staph}$ with good reactivity was obtained.

2.3. Sortase FRET activity assay

Sortase A substrate Dabcyl-LPGTG-Edans (Anaspec, CA) was dissolved in the reaction buffer (300 mM Tris-HCl, pH = 7.5, 150 mM NaCl, 5 mM $CaCl_2$) and added at a final concentration of 10 μM. Peptide cleavage was monitored as an increase in fluorescence intensity over time at 460 nm (λ_{ex} = 360 nm) with a SynergyMx spectrometer (BioTek Instrument, VT). Reaction was carried out in sortase activity buffer in a volume of 100 μL at 25 °C with 12 μM $SrtA_{Staph}$, and 1 mM triglycine.

2.4. Sortase-mediated peptide oligomer synthesis

Reactions were carried out by combining 250 μM methyl ester peptides and 12 μM $SrtA_{Staph\ in}$ sortase buffer (300 mM Tris-HCl, pH = 7.5, 150 mM NaCl, 5 mM $CaCl_2$) and incubated at 37 °C for times indicated. At each time point, 20 μL aliquots were withdrawn, and reaction was quenched by adding 5 μL of 0.1% trifluoroacetic acid (TFA). The reaction aliquots were purified through $ZipTip_{C\text{-}18}$ column (Millipore) and loaded on the target plate for MALDI-TOF/TOF analysis.

2.5. MALDI –TOF/TOF MS

Peptide products in the reaction mixtures were analyzed via Matrix-Assisted Laser Desorption Ion-Time of Flight/Time of flight (MALDI-TOF/TOF) mass spectrometry. All MALDI mass spectra were acquired using a Bruker UltraFlextreme MALDI-TOF/TOF mass spectrometer (Bruker Daltonics). The instrument was used in reflector mode and acquisition was optimized for a mass range from 600 to 3000 Da. All measurements were done with constant laser power of 40. The matrix used was α-cyano-4-hydrocinnamic acid (10 mg/mL in 50% acetonitrile with 0.05% trifluoroacetic acid). Experiments were carried with fixed amount of exogenous internal standard (neurotensin, monoisotopic MW 1671.9) [19]. A total of 4500 laser shots were summed for each spectrum (each sample spot was irradiated at 9 random but evenly distributed locations with 500 shots per location). Relative signal intensities within MALDI mass spectra were compared to determine relative yield of a particular peptide product. Using intensities of peaks that correspond to reaction products, yields were estimated as, for example, $\%\ \text{monomer} = I_{monomer}/(I_{monomer} + \Sigma I_{dimeric\ species} + \Sigma I_{trimeric\ species} + \Sigma I_{tetrimeric\ species})$, where I is intensity. The values for tetramers were also added when applicable.

2.6. CD analysis

The CD spectra of peptides were recorded on Jasco J-710 spectropolarimeter. The CD spectra were scanned at 20 °C in a capped, quartz optical cell with a 1.0 mm path length. Data was collected from 250 to 190 nm at an interval of 1.0 [21] nm with an integration time of two seconds at each wavelength. Five to ten scans were averaged, smoothed and background-subtracted for each measurement.

2.7. Peptide self-assembly

Peptides were dissolved in 300 mM Tris-HCl buffer (pH = 7.5) containing 150 mM NaCl and 5 mM $CaCl_2$. Peptide solutions (250 μM) were applied onto the surfaces silicon wafers and incubated in a moisture environment at 37 °C overnight. After washing with deionized water, peptide samples on silicon wafers were coated with gold. Morphologies of peptide aggregates were studied using scan Auriga Modular CrossBeam workstation (Carl Zeiss Inc., Thornwood, NY). Formation of peptide aggregates in solution was estimated using a fluorescence probe 1-anilinonaphthalene-8-sulfonic acid (1,8-ANS) [20]. ANS (20 μM) fluorescence emission spectrum increase caused by peptide aggregration was recorded on a fluorescent Microplate Reader (Biotek Inc.) by setting excitation wavelength at 369 nm.

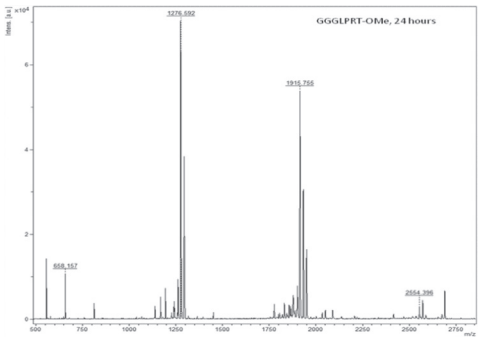

Peptides	Yield (%)									
	Monomer		Dimer		Trimer		Tetramer		Pentamer	
	Lin	Cyc	Lin	Cyc	Lin	Cyc	Lin	Cyc	Lin	Cyc
GGGLPRT	-	-	15	43	18	21	-	-	-	-
GGLPRT	-	-	-	-	7	62	5	25	-	-
GLPRT	-	-	-	-	-	32	9	47	5	11

Fig. 1. $SrtA_{Staph}$ mediated ligation and cyclization of short peptides containing one to three N-terminal glycines (Lin- Linear peptide/oliomer; Cyc-Cyclic peptide/oligomer). Top, typical MALDI TOF/TOF MS spectra from GGGLPRT-OMe; Bottom, calculated yields of different products. Reaction time: 24 h.

3. Results and discussions

We started our study on $SrtA_{Staph}$-mediated ultra-short peptide ligation using the minimal $SrtA_{Staph}$ recognization sequence based on publications, GGGLPRT-OMe, with a methyl ester at the C-termini. $SrtA_{Staph}$-catalyzed small peptide ligation was very efficient and 97% of GGGLPRT-OMe was converted into peptide oligomers at the end of 24 h reaction (Fig. 1). Resulting peptides were a mixture of dimers, trimers, tetramers, and pentamers in linear and cyclic forms, with dimer and trimer peptides as the main products.

Kinetic studies revealed that linear peptide oligomers formed early and rapidly (Fig. 2). Significant amounts of linear dimer, trimer, and tetramer were found after one hour of reaction when very low concentrations of corresponding cyclic oligomers were detected. However, the amount of cyclic oligomers increased as the reaction time was extended. There was a good dynamic correlation between linear oligomer disappearance and cyclic oligomer formation over the reaction period of 0–5 h. These data show that $SrtA_{Staph}$-catalyzed small peptide ligation includes two reactions: 1) formation of linear oligomers through the head-to-tail peptide ligation, and 2) cyclization of linear oligomers to form cyclic products by followed intramolecular transpeptidation. Interestingly, despite the quick accumulation of linear oligomers at the beginning of the reaction, linear oligomers in hydrolyzed forms (without methyl ester at the C-termini) were maintained at relatively stable levels within the first five hours of reaction. Increase of linear oligomers in hydrolyzed form was observed after a long time (> 5 h) reaction. There was good correlations between the formation of cyclic peptides and the production of corresponded linear peptides in the hydrolyzed forms, indicating the presence of $SrtA_{Staph}$-mediated ring opening reactions in cyclic oligomers. Oligomers containing more peptide units were especially prone to $SrtA_{Staph}$ mediated hydrolysis, and all GGGLPRT tetramers (both cyclic and linear) formed at the beginning of reactions disappeared at the end of 24-h reaction (Fig. 1).

It is known that the polyglycine sequence at the N-terminus of the

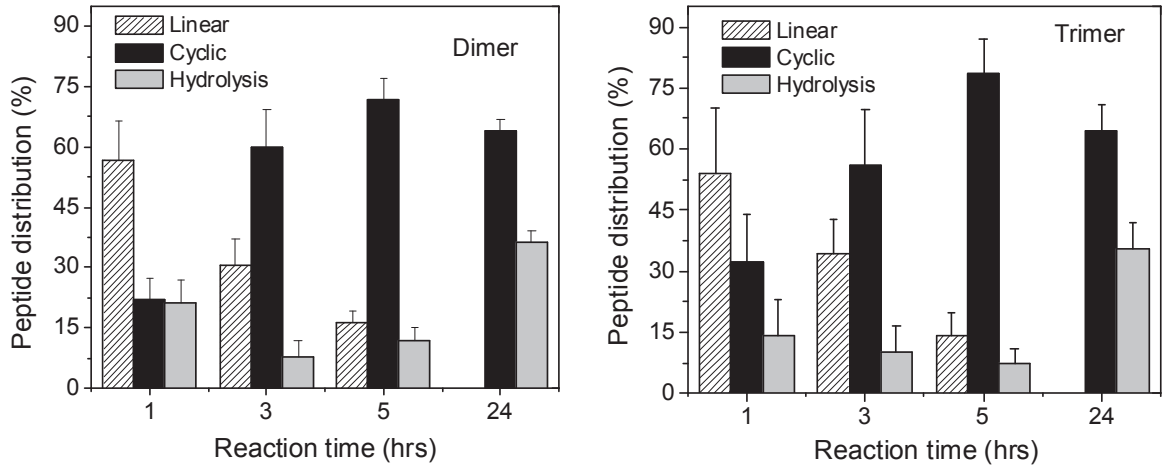

Fig. 2. Kinetics of dimer and trimer product formation in $SrtA_{Staph}$ catalyzed GGGLPRT-OMe ligation.

peptide can greatly affect $SrtA_{Staph}$ mediated protein ligation. Good reactive activity was usually observed for proteins/peptides with three or more glycine residues at N-terminus [22]. $SrtA_{Staph}$ mediated transpeptidation would not happen for proteins or peptides with only one N-terminal glycine [22,23]. To test the reactivity of $SrtA_{Staph}$ to small peptides with less than three N-terminal glycines, we extended our study to peptide GLPRT-OMe and GGLPRT-OMe. Both GLPRT-OMe and GGLPRT-OMe gave oligomer products (Fig. 2), indicating that a single aminoglycine was sufficient for nucleophilic attack at the small LPXT containing substrates. These results were in consistent with findings from recent studies [26,27]. However, significant differences in reaction kinetics and product distribution were found for GGGLPRT-OMe, GGLPRT-OMe, and GLPRT-OMe (Fig. 2): first, reactions of GLPRT-OMe and GGLPRT-OMe were associated with fewer amounts of linear oligomers. The sum of cyclic oligomers in the final products of GLPRT-OMe and GGLPRT-OMe reached 85%, which was higher than the 65% in GGGLPRT-OMe; second, $SrtA_{Staph}$-mediated ring-opening (hydrolysis) reaction was only observed for the cyclic products from GG GLPRT-OMe but not these from GLPRT-OMe or GGLPRT-OMe. Cyclic oligomers from GLPRT-OMe and GGLPRT-OMe increased steadily during the course of reaction (Fig. 3A & B). Obviously, LPRT-G or LPRT-GG linkages in cyclic oligomers from GLPRT-OMe and GGLPRT-OMe were not good substrates for $SrtA_{Staph}$ because the longer glycine linker limited the steric accessibility of the substrate to the active site, supporting the finding that LPXTG sequences containing three or more N-terminal glycines are good nucleophiles of $SrtA_{Staph}$ [22,23]; third, the main products for GLPRT-OMe and GGLPRT-OMe at the end of 24 h reaction were cyclic trimers and tetramers. Neither GLPRT-OMe nor G GLPRT-OMe formed a cyclic dimer, a main cyclic product of GGGLPRT-OMe. In contrast, cyclic pentamer was only found for GLPRT-OMe. Because GGGLPRT-OMe, GGLPRT-OMe, and GLPRT-OMe existed as random coils in solutions, potential contributions of peptide secondary structures to $SrtA_{Staph}$-mediated small peptide ligation could be excluded. Kinetic results suggested that linear dimers did exist at the early phase of GLPRT-OMe and GGLPRT-OMe reactions (Fig. 3C & D) but they failed to procede intramolecular transpeptidation to form cyclic products. We know that side chain interactions among amino acid residues in cyclic peptides will be much stronger than those in linear ones. Therefore, the strong ring stain might explain why dimers were the main cyclic oligomer for GGGLPRT-OMe but not for GLPRT-OMe and GGLPRT-OMe. Data from GLPRT-OMe, GGLPRT-OMe and GG GLPRT-OMe (Fig. 1) suggest that peptide lengths had dramatic effects on the final products of $SrtA_{Staph}$-mediated small peptide ligations.

The important role of peptide length in $SrtA_{Staph}$-catalyzed small peptide cyclization was confirmed by using small peptides with increased peptide lengths (7–10 amino acids) but containing only one N-terminal glycine (G*HKL*PRT-OMe, GHHPHLPRT-OMe, and GVPGVGLPRT-OMe) (Fig. 4). Like other small peptides, all three selected peptides do not have specific secondary structures and exist as random coils in solutions (Fig. 4, top). Cyclic peptides were also the main products (yield > 81%) for all three peptides. Peptide lengths had the same effect on $SrtA_{Staph}$-catalyzed peptide ligation: cyclic dimers were major products of GHHPHLPRT-OMe and GVPGVGLPRT-OMe but were not found for G*HKL*PRT-OMe (Fig. 4, bottom).

$SrtA_{Staph}$-mediated small peptide ligations are summarized in Fig. 5. $SrtA_{Staph}$ catalyzed small peptides to form linear peptide oligomers efficiently (yield > 85%) and rapidly (< 60 min). However, $SrtA_{Staph}$ was unable to position both ends of small peptide oligomers (less than 14 amino acids) in a productive binding arrangement for the intramolecular amide bond to form cyclic oligomers because of steric hindrance. However, once bigger peptide oligomers were formed, they would undergo intramolecular transpeptidation to form cyclic products. $SrtA_{Staph}$ catalyzed cyclization was slow in comparison with linear oligomerization, and might take hours to complete. Because adding extra peptide units to large oligomers would become more difficult and oligomers containing multiple copies of G-LPRT sequences became prone to $SrtA_{Staph}$ hydrolysis, peptide oligomers (both linear and cyclic) with more than 30 amino acids were hardly synthesized from small (< 10 amino acid in length) peptides. On the contrary, once formed, the small ring formed by shorter peptides will have strong steric hindrance and thus cannot readily adopt a conformation to rebind to SrtA for hydrolysis. Therefore, only middle sizes (15–30 amino acid residues) of cyclic peptides formed in SrtA catalyzed small peptide ligation.

An interesting question was what would be the products of peptides with more than 15 amino acids. Such peptides met the minimal length requirement (> 14 amino acids) for cyclization but even dimers of these peptides would exceed the length limit (< 30 amino acids) to generate stable ligation products. We tested $SrtA_{Staph}$ catalyzed peptide ligation on a 19-aa peptide (GGGWLGALFKALSKLLPRT-OMe). As we had expected, oligomers from this peptide were not found. However, high yield (~83%) and single cyclic product from the direct cyclization of GGGWLGALFKALSKLLPRT-OMe was produced (Fig. 4, Bottom).

There has been an increased interest and rapid expansion in the study of cyclic peptides over the last decade. Strategies for synthesizing cyclic peptides include side chain to side chain, side chain to terminal group, and terminal group to terminal group (head-to-tail) cyclization. These methods, however, are inefficient for cyclization of large peptides (> 10 residues) due to the large entropic barriers for such reactions and competing intermolecular oligomerization. Findings from this study provide useful information to the synthesis of linear and cyclic oligomers from ultra-short peptides for wide pharmaceutical and biomedical applications. We know that cyclic peptides may have other advantages over their linear counterparts due to their unusual biological activity, improved thermodynamic stability, and increased resis-

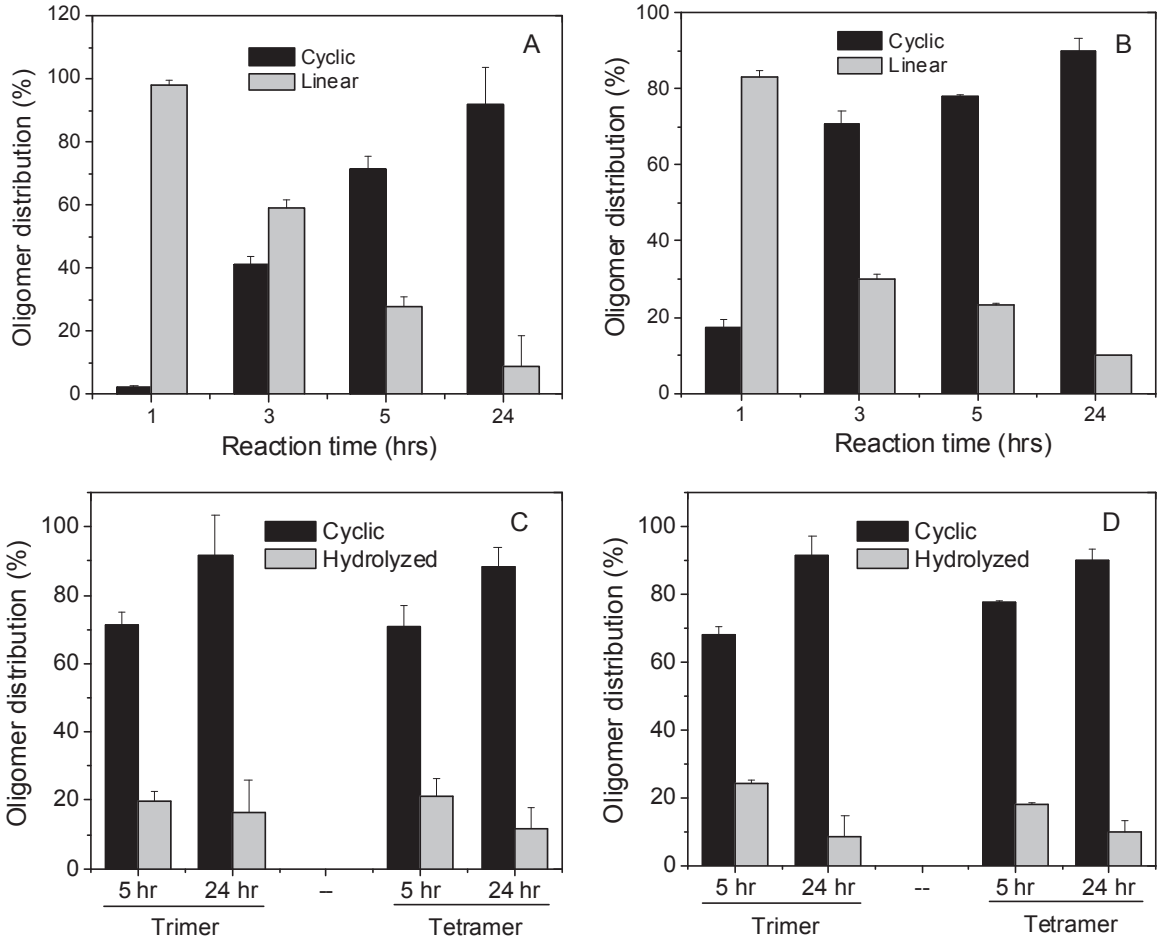

Fig. 3. A & B) Kinetics of $SrtA_{Staph}$-catalyzed transpeptidation of GLPRT-OMe (A) and GGLPRT-OMe(B); C & D) Comparison of cyclic and hydrolyzed products in the reaction mixtures of GLPRT-OMe (C) and GGLPRT-OMe (D) at end of 5 and 24 h reactions. Data represent relative amount of a product in the reaction mixture at the specific time point.

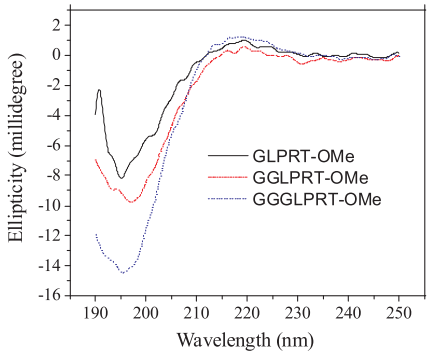

Peptides	Yield (%)			
	Monomer	Dimer	Trimer	Tetramer
GHKLPRT	-	-	54	27
GHHPHLPRT	-	38	52	-
GVPGVGLPRT	-	60	24	-
GGGWLGALFKALSKLLPRT	83	-	-	-

Fig. 4. $SrtA_{Staph}$ mediated ligation and cyclization of peptides of different lengths. Top, CD spectra of peptides; Bottom, calculated yields of products from $SrtA_{Staph}$-catalyzed transpeptidation.

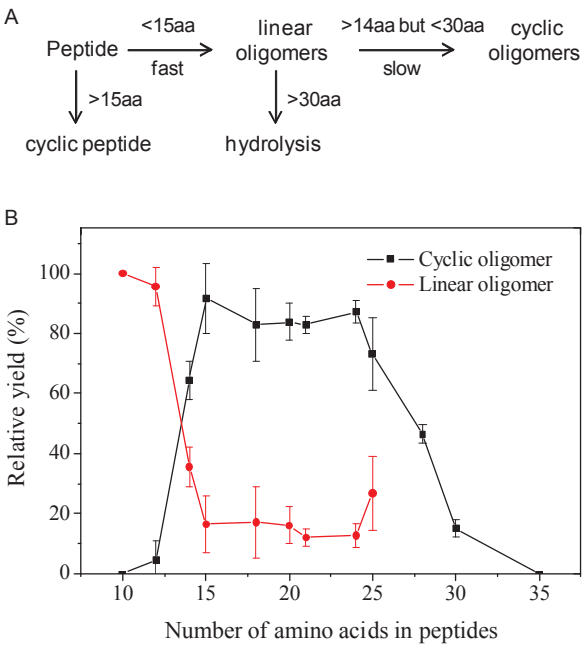

Fig. 5. A) Summary of $SrtA_{Staph}$-catalyzed ultra-short peptide oligomerization; B) Peptide lengths affected the products from $SrtA_{Staph}$-catalyzed peptide ligation. Relative yields were calculated for the reaction products detected at 24 h. Cyclic yield (%) = cyclic products/(cyclic products + linear products).

tance to protease digestion [24,28,29]. In addition, nano-structured surfaces and scaffolds are essential for assisting bone and neuron cell growth and have a wide range of biomedical applications [30,31]. Peptides or peptide oligomers with specific sequences can also self-assemble to form materials with regular nanostructures and demonstrate unusual stability [7,8]. Because of good biocompatibility, biomaterials using self-assembled peptides instead of synthetic polymers

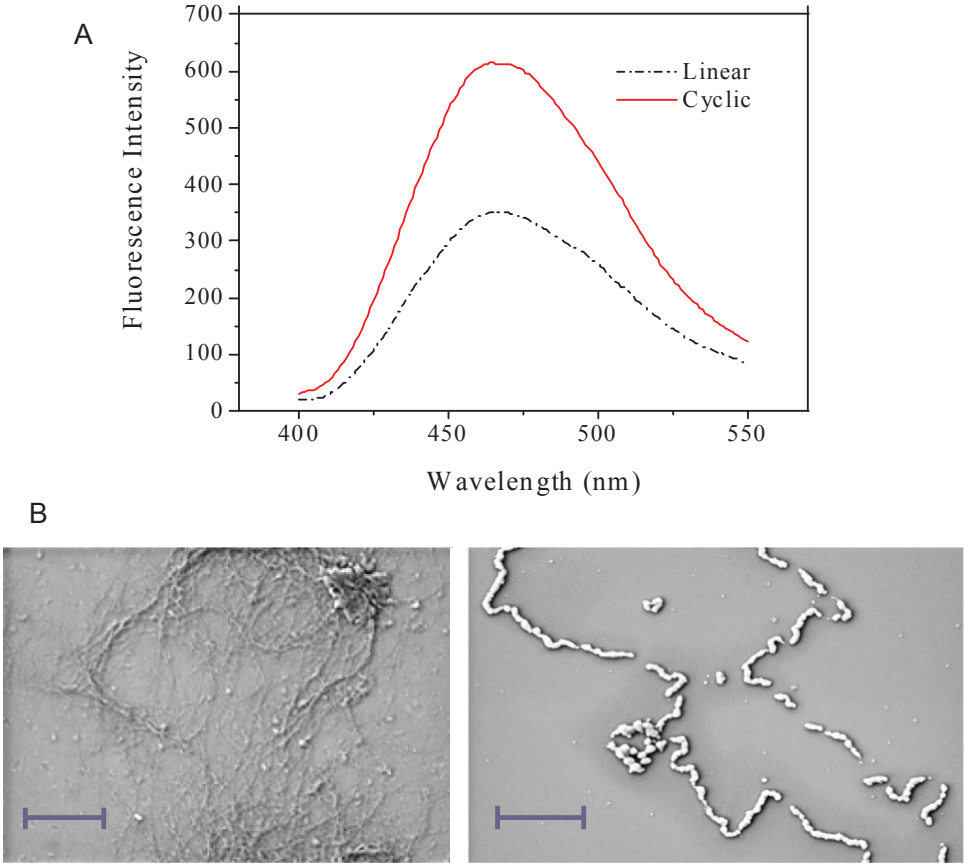

Fig. 6. Changed self-assembling properties of linear and cyclic GGGWLGALFKALSKLLPRT peptides. A) Self-assembly of linear and cyclic peptides in solutions as confirmed using fluorescence probe 1,8-ANS; B) Typical structures of self-assembled linear (left) and cyclic (right) peptides in DI water as visualized using SEM. Scale bar = 1.0 μm.

have been generated recently [32,33]. Taking peptide GGGWLGALFKALSKLLPRT-OMe as an example: although both linear and cyclic peptide self-assembled in water, they behaved differently (Fig. 6A) and formed peptide aggregates with distinct super-molecular structures (Fig. 6B).

Acknowledgements

This work was partially supported by NIH grant GM081874.

Appendix A. Transparency document

Supplementary data associated with this article can be found in the online version at doi:10.1016/j.bbrep.2017.02.005.

References

[1] G. Zhang, X. Yin, Y. Qi, L. Pendyala, J. Chen, D. Hou, C. Tang, Ghrelin and cardiovascular diseases, Curr. Cardiol. Rev. 6 (2010) 62–70.
[2] G.L. Bidwell, Peptides for cancer therapy: a drug-development opportunity and a drug-delivery challenge, Ther. Deliv. 3 (2012) 609–621.
[3] L.T. Nguyen, E.F. Haney, H.J. Vogel, The expanding scope of antimicrobial peptide structures and their modes of action, Trends Biotechnol. 29 (2011) 464–472.
[4] S. Kihara, H. Takagi, K. Takechi, K. Takeda, Chelation of transition metal ions by peptide nanoring, J. Phys. Chem. B 112 (2008) 7631–7644.
[5] H. Hua, L. Münter, A. Harmeier, O. Georgiev, G. Multhaup, W. Schaffner, Toxicity of Alzheimer's disease-associated Aβ peptide is ameliorated in a Drosophila model by tight control of zinc and copper availability, Biol. Chem. 392 (2011) 919–926.
[6] M. Jelokhani-Niaraki, L.H. Kondejewski, L.C. Wheaton, R.S. Hodges, Effect of ring size on conformation and biological activity of cyclic cationic antimicrobial peptides, J. Med. Chem. 52 (2009) 2090–2097.
[7] B.J. Pepe-Mooney, B. Kokona, R. Fairman, Characterization of mesoscale coiled-coil peptide-porphyrin complexes, Biomacromolecules 12 (2011) 4196–4203.
[8] V. Setnicka, J. Hlavácek, M. Urbanová, Cationic oligopeptides with the repeating sequence L-lysyl-L-alanyl-L-alanine: conformational and thermal stability study using optical spectroscopic methods, J. Pept. Sci. 15 (2009) 533–539.
[9] U. Ilangovan, H. Ton-That, J. Iwahara, O. Schneewind, R.T. Clubb, Structure of sortase, the transpeptidase that anchors proteins to the cell wall of Staphylococcus aureus, Proc. Natl. Acad. Sci. USA 98 (2001) 6056–6061.
[10] B.M. Dorr, H.O. Ham, C. An, E.L. Chaikof, D.R. Liu, Reprogramming the specificity of sortase enzymes, Proc. Natl. Acad. Sci. USA 111 (2014) 13343–13348.
[11] D.J. Williamson, M.E. Webb, W.B. Turnbull, Depsipeptide substrates for sortase-mediated N-terminal protein ligation, Nat. Protoc. 9 (2014) 253–262.
[12] M.W. Popp, J.M. Antos, G.M. Grotenbreg, E. Spooner, H.L. Ploegh, Sortagging: a versatile method for protein labeling, Nat. Chem. Biol. 3 (2007) 707–708.
[13] T. Tanaka, T. Yamamoto, S. Tsukiji, T. Nagamune, Site-specific protein modification on living cells catalyzed by Sortase, Chembiochem. 9 (2008) 802–807.
[14] Z. Wu, X. Guo, Q. Wang, B.M. Swarts, Z. Guo, Sortase A-catalyzed transpeptidation of Glycosylphosphatidylinositol derivatives for chemoenzymatic synthesis of GPI-anchored proteins, J. Am. Chem. Soc. 13 (2010) 1567–1571.
[15] D.J. Williamson, M.A. Fascione, M.E. Webb, W.B. Turnbull, Efficient N-terminal labeling of proteins by use of sortase, Angew. Chem. Int. Ed. 51 (2012) 9377–9380.
[16] M.W. Popp, H.L. Ploegh, Making and breaking peptide bonds: protein engineering using sortase, Angew. Chem. Int. Ed. 50 (2011) 5024–5032.
[17] J. Touati, A. Angelini, M.J. Hinner, C. Heinis, Enzymatic cyclisation of peptides with a transglutaminase, ChemBioChem 12 (2011) 38–42.
[18] J.M. Antos, G.L. Chew, C.P. Guimaraes, N.C. Yoder, G.M. Grotenbreg, M.W. Popp, H.L. Ploegh, Site-specific N- and C-terminal labeling of a single polypeptide using sortases of different specificity, J. Am. Chem. Soc. 131 (2009) 10800–10801.
[19] Z. Tu, M. Volk, K. Shah, K. Clerkin, J.F. Liang, Constructing bioactive peptides with pH-dependent activities, Peptides 30 (2009) 1523–1528.
[20] L. Chen, J.F. Liang, Peptide fibrils with altered stability, activity, and cell selectivity, Biomacromolecules 14 (2013) 2326–2331.
[21] L. Chen, N. Patrone, J.F. Liang, Peptide self-assembly on cell membranes to induce cell lysis, Biomacromolecules 13 (2012) 3327–3333.
[22] L. Chan, H.F. Cross, J.K. She, G. Cavalli, H.F. Martins, C. Neylon, Covalent attachment of proteins to solid supports and surfaces via Sortase-mediated ligation, PLoS One 2 (2007) e1164.
[23] X. Huang, A. Aulabaugh, W. Ding, B. Kapoor, L. Alksne, K. Tabei, G. Ellestad, Kinetic mechanism of Staphylococcus aureus sortase SrtA, Biochemistry 42 (2003) 11307–11315.
[24] A.S. Andersen, E. Palmqvist, S. Bang, A.C. Shaw, F. Hubalek, U. Ribel, T. Hoeg-Jensen, Backbone cyclic insulin, J. Pept. Sci. 16 (2010) 473–479.
[25] Z. Wu, X. Guo, Z. Guo, Sortase A-catalyzed peptide cyclization for the synthesis of macrocyclic peptides and glycopeptides, Chem. Commun. 47 (2011) 9218–9220.
[26] B.M. Paterson, K. Alt, C.M. Jeffery, R.I. Price, S. Jagdale, S. Rigby, C.C. Williams, K. Peter, C.E. Hagemeyer, P.S. Donnelly, Enzyme-mediated site-specific bioconju-

gation of metal complexes to proteins: sortase-mediated coupling of copper-64 to a single-chain antibody, Angew. Chem. Int. Ed. 53 (2014) 6115–6119.
[27] D.J.1 Williamson, M.A. Fascione, M.E. Webb, W.B. Turnbull, Efficient N-terminal labeling of proteins by use of sortase, Angew. Chem. Int. Ed. 51 (2012), pp. 9377–9380.
[28] R.J. Clark, J. Nevin Jensen, S.T. Callaghan, B.P. Adams, D.J. Craik, D. J, Angew. Chem. Int. Ed. Engl. 49 (2010) 6545.
[29] D.J. Craik, Science 311 (2006) 1563.
[30] M.R. Abidian, K.A. Ludwig, T.C. Marzullo, D.C. Martin, D.R. Kipke, Adv. Mater. 21 (2009) 3764–3770.
[31] M.R. Abidian, J.M. Corey, D.R. Kipke, D.C. Martin, Small 6 (2010) 421–429.
[32] G. Cinar, H. Ceylan, M. Urel, T.S. Erkal, E. Deniz Tekin, A.B. Tekinay, A. Dâna, M.O. Guler, Biomacromolecules 13 (2012) 3377–3387.
[33] A. Mujeeb, A. Saiani, J.E. Gough, Acta Biomater. (2012) S1742–S7061.